Source: Heinrich I, Gärtner H, Monbaron M, Schleser G (eds.) (2006) TRACE - Tree Rings in Archaeology, Climatology and Ecology, Vol. 4: Proceedings of the DENDROSYMPOSIUM 2005, April 21st – 23rd 2005, Fribourg, Switzerland. Schriften des Forschungszentrums Jülich, Reihe Umwelt Vol. 61, p. 23 – 30.

Mean sea level pressure composite mapping as an exploratory tool in dendroclimatology

A. Fowler

School of Geography and Environmental Science, The University of Auckland, Private Bag 92019, Auckland New Zealand. Email: a.fowler@auckland.ac.nz

Introduction

A typical starting point in dendroclimatological research is to statistically relate tree-ring growth indices to local or regional climate variables (response function analysis). This sometimes leads to identification of links between tree growth and perturbations in atmospheric circulation, the latter often oscillatory in nature, such as the El Niño - Southern Oscillation (ENSO) phenomenon. This approach relies on the researcher linking the (hopefully known) local-scale climate impacts of an oscillatory phenomenon with the response function results. An alternative is to directly investigate relationships between tree growth and atmospheric circulation using composite mapping techniques. Here I explain and demonstrate composite mapping, using the United Kingdom Meteorological Office gridded global monthly mean sea level pressure data set (GMSLP2.1f) and *Agathis australis* (kauri) tree rings.

Data

Gridded Pressure

Although the mapping of global MSLP has a long history, digital gridded MSLP data sets covering significant portions of the globe (required for the compositing analysis presented here) are a relatively recent development (Barnett et al. 1984; Harnack and Harnack 1984; Jones and Wigley 1988; Jones et al. 1987; Jones 1991). The methods used to develop these have evolved considerably over the last twenty years (e.g. establishing background climatology, spatial interpolation techniques, error detection and correction), but the basic requirement of reconstructing a spatial grid from incomplete point data is common.

By the mid-1990s, attempts were being made to combine regional gridded data sets, such as that of Jones (1991), to produce a full global domain. One result of these activities was the United Kingdom Meteorological Office GMSLP2 data set used by Allan et al. (1996) to investigate global MSLP patterns associated with the El Niño – Southern Oscillation (ENSO) phenomenon. Blending diverse regional gridded data sets was a complex exercise, having to deal with a myriad of additional problems, such as: differences in grids and time periods; differences in how missing data was dealt with; and spatial inhomogeneities between data sets (Basnett and Parker 1997). Several versions of GMSLP2 were produced as methods developed, including the direct incorporation of observed data to supplement the blended gridded data (Basnett and Parker 1997). GMSLP2.1f is the version of the data set used here.

GMSLP2.1f is a gridded 5° latitude by 5° longitude fully global monthly MSLP data set for the period 1871 to 1994. Basnett and Parker (1997) evaluated GMSLP2.1f. They note that the inclusion of quality-controlled observed data (since GMSLP2.1a) has improved reliability, but they also identify several weaknesses. These include the need to resort to climatology in data sparse regions, especially in the Southern Hemisphere prior to 1951, and a lack of reliability in earlier decades.

Kauri tree rings

The proxy data used here is the modern kauri master chronology (AGAUm04a) built by Fowler et al. (2004). Fowler et al. provided details of kauri, the data used to build the chronology, and the chronology construction method. For the 1871-1994 period (corresponding to GMSLP2.1f), the kauri master was built from at least 145 trees from 15 sites, growing throughout kauri's natural growth range in the far north of New Zealand (north of 38S). Fowler et al. standardised the kauri tree ring width time series used to build the master using very flexible smoothing splines (50% variance cut-off at 20 years). The standardisation maximised the climate signal in kauri by removing radii- and tree-specific "noise", resulting in a master tree-ring chronology with utility for investigating high frequency climate forcing, but lacking multi-decadal to century scale information.

Southern Oscillation Index (SOI)

The ENSO component of this research was limited to the most commonly used index of the SO, the normalised pressure difference between Tahiti and Darwin. These are relatively long-term surface air pressure recording sites, near the respective poles of the SO across the equatorial Pacific Ocean. Specifically, monthly SOI values (1871–1994) published on the Internet by CSIRO Division of Atmospheric Research were used. These values are relative to a 1933–1992 base period.

Auckland Drought Index

Fowler and Adams (2004) modelled soil water for Auckland using a daily soil water balance model. Model details were presented by Fowler (1999) and application for long-term soil water modelling was described by Fowler (2002). Fowler and Adams (2004) computed monthly mean soil water deficits and used a 1900–1994 subset for MSLP composite mapping. The same data set is used here.

Composite Mapping

Composite mapping is a technique used by climatologists to identify consistent spatial patterns in relationships. For example, Allan et al. (1996) investigated the global-scale fingerprint of ENSO by mapping common responses (frosts, fires, temperature, precipitation, etc) to past El Niño and La Niña events. When applied to gridded MSLP data, compositing involves looking for patterns within the MSLP fields, typically expressed in terms of anomalies relative to some reference period. These anomaly fields are then interpreted in terms of associated impacts on the frequency and/or strength of prevailing winds, which in turn may help explain observed statistical relationships.

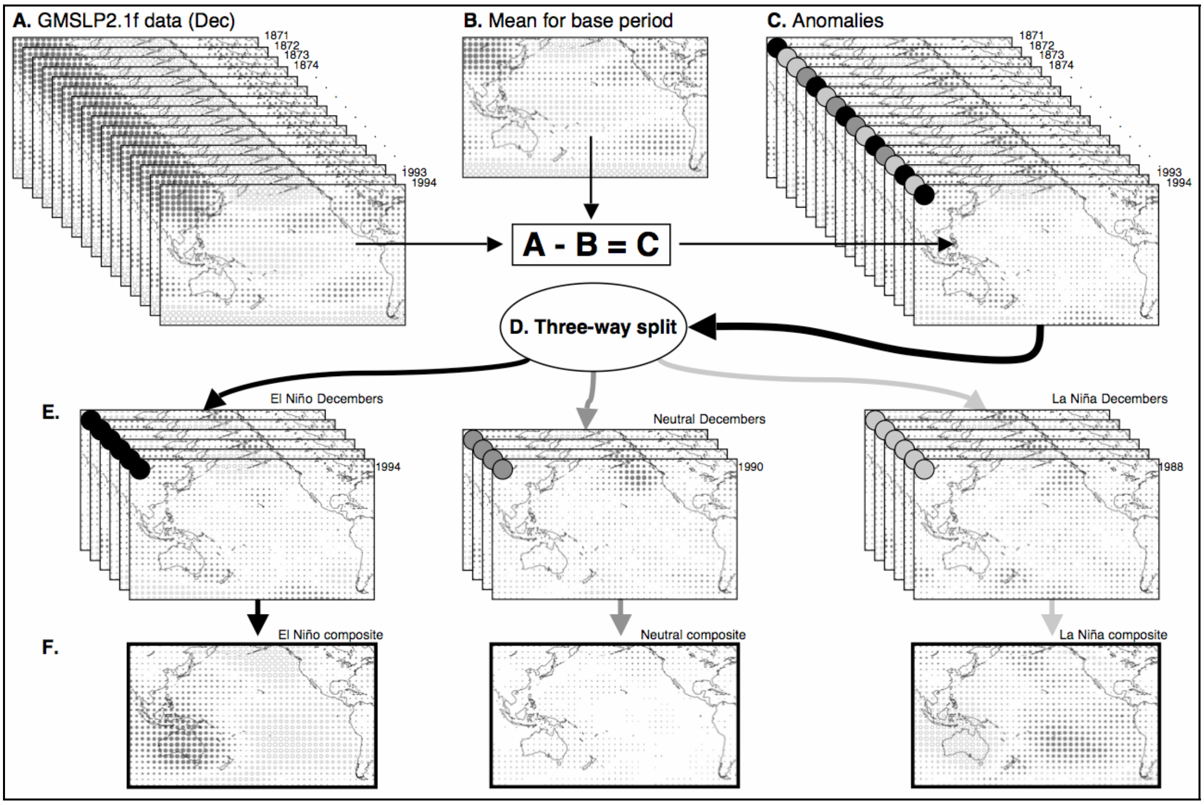

Figure 1: Schematic representation of composite mapping using a card stack analogy. Solid (open) dots indicate MSLP above (below) standard atmospheric pressure at sea level (A, B), or positive (negative) MSLP anomalies (C, E, F). Dot area indicates magnitude (±30 hPa for A, B, C, E; ±3 hPa for F). Shaded dots in the top left corners of stacks in C and E indicate the way cards are split (based on a compositing key variable).

Figure 1 is a schematic representation of composite mapping, as applied to the GMSLP2.1f data set, using the analogy of a stack of cards. December is used here to demonstrate the method for a subset of the global domain, centred on the Pacific Ocean. The same method would be repeated for other months and results subsequently combined into time periods of interest (e.g. seasons or longer multi-month blocks). Starting from the 1488 monthly cards in the GMSLP2.1f data set, through to interpretation of the composite spatial anomaly fields, can be viewed as the nine-step process outlined below.

Figure 1A represents the full set of GMSLP2.1f data for December (124 cards). The dots on the top card show the data grid. Solid (open) dots indicate MSLP above (below) standard atmospheric pressure at sea level (1013.25 hPa), with the area of the dots indicating the magnitude of the departure (ca. ±30 hPa). For the purpose of this demonstration the full set of cards is used for compositing. However, because of the quality issues previously outlined, it may be appropriate to limit analysis to a high quality period (e.g. 1951-1994). Some research questions may also require the use of temporal subsets, or even multiple subsets where evolving patterns are being investigated. Splitting the pressure data into monthly sub-stacks is the first step in composite mapping. Determining the temporal subset(s) to use is the second.

Several broad scale features are apparent in Figure 1A which characterise the atmospheric circulation in December. These include the Siberian High in the northwest corner, the Aleutian Low in the north Pacific, equatorial low pressure, high pressure ridges either side of the equator, and the low pressure band in the south. These features are a function of the annual cycle and are therefore common to all cards in the December stack. Differences between Decembers are subtle changes in the relative strength of the features and small shifts in position. Consequently, when an average is computed for the stack (Fig. 1B), the common features come through strongly. Computation of this gridded mean field is the third compositing step, calculated over the entire temporal subset, or for a more restricted base period (e.g. 1961-90). The latter is particularly appropriate where a comparison is being made with other data sets where a reference base line period has been used, such as the SOI.

The fourth step is the calculation of gridded pressure anomaly fields (Fig. 1C). This is simply the mean fields subtracted from the original pressure data for each month. This generates a new stack of gridded pressure field “anomalies” relative to normal conditions which shows the magnitude and spatial extent of anomalous MSLP features. Solid (open) dots now indicate positive (negative) pressure anomalies. In the case of December 1994, the anomaly field (Fig. 1C) shows a strengthening of both the Siberian High and the Aleutian Low, with much of the eastern Pacific rim experiencing higher than normal pressure. All subsequent analyses use the anomalies data set.

The primary purpose of composite mapping is to investigate if there are consistent patterns in MSLP anomaly fields associated with potential forcing factors or some consequent impact. For example, compositing based on sea-surface temperatures in the NINO3.4 region of the equatorial Pacific could reveal MSLP anomalies (which may or may not be forced) associated with ENSO events. Conversely, compositing based on local drought may indicate persistent pressure anomalies forcing local climate variation. To do the compositing, a relevant “compositing key” variable is used to make a three-way split of the gridded anomalies stack (Fig. 1D). Monthly or annually resolved compositing keys can be used and the three-way split can be into equal or unequal sub-stacks (Fig. 1E). Three-way splitting of the data is the fifth compositing step.

The sixth step is calculation of mean gridded MSLP for each of the three composites (Fig. 1F). This is intended to bring out any common spatial pattern associated with the compositing key. The example shown in Figure 1 is for ENSO-based compositing. Cards in the left stack of Figure 1E are Decembers during El Niño years (including December 1994), cards in the right stack are Decembers during La Niña years (including December 1988), and the middle stack is for all other Decembers (including December 1990). Averaging through the El Niño composite cards gives the characteristic MSLP anomaly pattern for El Niños of high pressure over Australia, extending into Southeast Asia and the Indian Ocean, with a boomerang-shaped low pressure anomaly field in the eastern Pacific. The La Niña composite shows a near-opposite pattern, and no significant anomaly pattern is associated with the

ENSO-neutral composite. Note though that there is an order of magnitude change in the scale of the anomalies plotted in Figure 1F. Whereas December anomalies for 1988 (La Niña), 1990 (ENSO-neutral) and 1994 (El Niño) are ±21 hPa, the mean anomalies for the El Niño and La Niña composites are less than 2 hPa. Clearly the patterns emerging from the compositing analysis are subtle relative to inter-annual variability, at least in terms of monthly data.

The seventh step is to numerically combine (e.g. by averaging) monthly plots, such as those shown in Figure 1F, into multi-month blocks of interest (e.g. seasons). These are then plotted (Step 8, Fig. 1F). If spatial patterns in the composite maps are apparent, these are then interpreted in terms of altered wind fields and associated local climate effects (Step 9). For example, in the case of the El Niño composite, the positive pressure anomalies over Australia indicate more frequent and/or more intense high pressure systems, bringing an increased chance of drought. They also indicate more frequent and/or stronger southerly quarter winds over New Zealand, resulting in cooler conditions, but a complex precipitation response (due to interactions with New Zealand's complex topography).

A Kauri Example

The discussion to this point has systematically summarised a standard climatological analysis technique. This section is a novel application of that technique to a high resolution climate proxy. The intention is to demonstrate how composite mapping can be used to identify the climate reconstruction potential of a proxy.

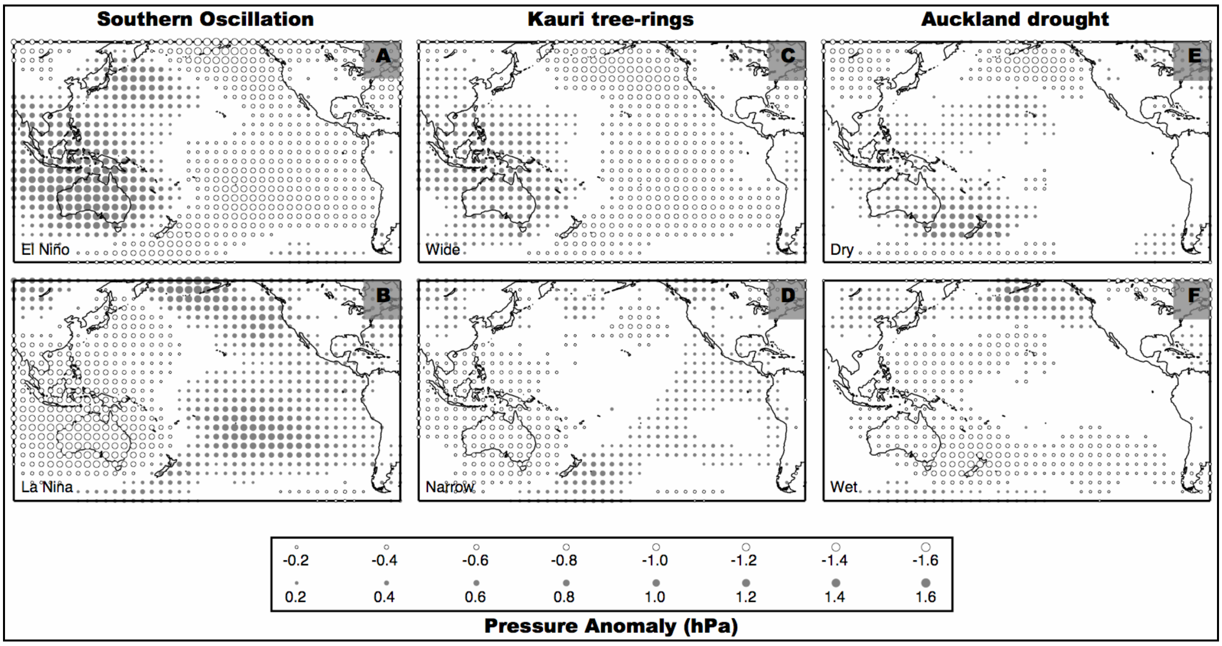

Figure 2: September to February MSLP anomaly composite maps for three compositing key variables (SOI, kauri tree-ring indices, Auckland drought). Composites were calculated for the common period 1901-1994 with equal three-way splits into composite stacks (only high and low composites shown).

Figure 2 shows compositing results derived from a 1901-1994 subset of GMSLP2.1f for three compositing key variables (SOI, kauri tree-ring indices, Auckland drought). The analyses were limited to the six month window from September to February, based on known persistent negative correlations between kauri tree-ring indices and local monthly precipitation and surface air temperature over this interval (Buckley et al. 2000). The 1901-1994 time period was determined by the limit of the available drought index data (Fowler and Adams 2004). Auckland has the longest record of climate data within kauri's growth range, and is conveniently close to the middle of that range (see Fowler et al. (2004) for details).

The SOI and drought analyses were based on monthly compositing, in which each month was separated into three stacks based on the composite key value for that specific month. This is as described in Section 3. For kauri, however, there was only one index value for each year, so the compositing was done based on whole six month blocks. For example, if the tree-ring index for a given year corresponded to a high composite (wide ring), then each month from September to February was allotted to a high composite stack. Equal three-way splitting of the months was done for each compositing key.

MSLP composite maps for wide and narrow kauri tree rings (Fig. 2C, D) indicate Pacific Basin wide relationships. Wide rings are associated with positive anomalies over South-east Asia and Australia; and also with negative anomalies extending in a boomerang shape from the northern central, through the eastern, to the southern central Pacific (south and east of New Zealand). Narrow rings show close to a near-reversal of the anomaly patterns in a band extending from the South-east Asian archipelago to the southern ocean, southeast of New Zealand. A weaker reversal to positive pressure anomalies is also apparent in the eastern Pacific, but this breaks down in the northern Pacific.

The kauri growth region in the far north of New Zealand lies between the pressure anomaly features centred over Australia and Indonesia, and those (of opposite sign) to the southeast of New Zealand. This means that wide and narrow kauri tree rings are associated with significant and opposite wind field perturbations. For example, in the case of wide rings, the pressure anomaly fields shown in Fig. 2C would be expected to cause an increase in the frequency and/or strength of south-westerly winds, bringing relatively cool and dry conditions. The associated pressure anomaly fields for narrow rings would be expected to result in warmer and wetter conditions.

The MSLP composite maps for kauri contrast with those for Auckland dry and wet phases (Fig. 2E, F). The latter demonstrate some spatially extensive anomaly patterns, but the most obvious features are synoptic-scale patterns straddling New Zealand. In contrast, the kauri composite maps exhibit strong similarity to those corresponding to ENSO phases (Fig. 2A, B). The agreement between the El Niño composite map (Fig. 2A) and that for kauri wide rings (Fig. 2C) is particularly striking. The kauri wide-ring anomalies are weaker and there is no significant high pressure anomaly east of Japan, but the patterns are otherwise nearly identical, especially in the Australasian region (including the demarcation between positive and negative anomalies). Anomaly patterns associated with narrow rings (Fig. 2D) agree well with the La Niña composite (Fig. 2B) in a band from Indonesian extending through to the southeast of New Zealand, but the representation of the La Niña phase positive eastern Pacific anomaly pattern is weaker, especially in the north Pacific.

Clearly, kauri has rather more potential as an ENSO proxy than as a drought proxy. The fact that the best agreement is between wide rings and El Niño suggests that kauri may have greater value as an El Niño than a La Niña proxy. It may also provide a better representation of the western than eastern pole of the SO.

Conclusions

The results show that composite mapping is a powerful tool for tree-ring research, capable of identifying atmospheric circulation characteristics associated with wide and narrow tree rings, and helping to determine the potential of tree rings for reconstructing atmospheric circulation features. Note though that the example presented here is very limited. A more detailed compositing-based analysis of the relationship between kauri growth and ENSO in Fowler (2005) shows additional applications in stationarity and sensitivity analyses, and to refining understanding of tree growth response to forcing. Fowler (2005) also discusses some of the pitfalls of composite mapping.

References

Allan, R.J., Lindesay, J.A., Parker, D.E. (1996): El Niño Southern Oscillation and Climatic Variability. CSIRO Publications, Melbourne. pp. 405.

Barnett, T.P., Brennecke, K., Limm, J., Tubbs, A.M. (1984): Construction of a near-global sea-level pressure field. Scripps Institute of Oceanography, La Jolla, CA, *SIO Reference Series* 84-7.

Basnett, T., Parker, D. (1997): Development of the Global Mean Sea Level Pressure Data Set GMSLP2, *Climate Research Technical Note 79*, Hadley Centre, United Kingdom Meteorological Office.

Buckley, B., Ogden, J., Palmer, J., Fowler, A., Salinger, J. (2000): Dendroclimatic interpretation of tree-rings in Agathis australis (kauri). 1. climate correlation functions and master chronology. *J Roy Soc NZ 30*: 263-275.

Fowler, A.M. (1999): Potential climate change impacts on water resources in the Auckland Region (New Zealand). *Clim Res 11*, 221-245.

Fowler, A.M. (2002): Assessment of the validity of using mean potential evaporation in computations of the long-term soil water balance. *J Hydrol 256*, 248-263.

Fowler, A.M. (2005): Sea-level pressure composite mapping in dendroclimatology: advocacy and an *Agathis australis* (kauri) case study. *Clim Res* 29, 73-84.

Fowler, A., Adams, K. (2004): Twentieth century droughts and wet periods in Auckland (New Zealand) and their relationship to ENSO. *Int J Climatol* 24: 1947–1961.

Fowler, A., Boswijk, G., Ogden, J. (2004): Tree-ring studies on Agathis australis (kauri): a synthesis of development work on Late Holocene chronologies. *Tree-Ring Res 60*:15-29.

Harnack, J., Harnack, R.P. (1984): A Southern Hemisphere sea level pressure data set for use in climate studies. *J Climatol 4*: 187-204.

Jones, P.D. (1991): Southern Hemisphere sea level pressure data: an analysis and reconstructions back to 1951 and 1911. *Int J Climatol 11*: 585-607.

Jones, P.D., Wigley, T.M.L. (1988): Antarctic gridded sea level pressure data: an analysis and reconstruction back to 1957. *J Clim 1*: 1199–1220.

Jones, P.D., Wigley, T.M.L., Briffa, K.R. (1987): Monthly mean pressure reconstructions for Europe (to 1780) and North America (to 1858). US Department of Energy Carbon Dioxide Research Division, Washington DC *DoE Technical Report TR037*, p 99.